Supporting Information

Potential-resolved electrochemiluminescence resonance energy transfer strategy for simultaneous detection of neuron-specific enolase and cytokeratin 19 fragment

Guichun Mo, Xuanming He, Dongmiao Qin, Xiaohua Jiang, Xiangfei Zheng and Biyang Deng*

State Key Laboratory for the Chemistry and Molecular Engineering of Medicinal Resources, School of Chemistry and Pharmaceutical Sciences, Guangxi Normal University, Guilin 541004, China

*Corresponding Author:

Telephone: +86-773-5845726; Fax: +86-773-2120958. Email: dengby16@163.com

Table of Contents

Experimental Section

Reagents. Thioacetamide (TAA), tin tetrachloride pentahydrate ($SnCl_4 \cdot 5H_2O$), polyethylene glycol (PEG), sodium citrate, 1-ethyl-3-(3-dimethylaminopropyl) carbodiimide (EDC), N-hydroxysuccinimide (NHS), oxalic acid, hexadecyl trimethyl ammonium bromide (CTAB), H_2PtCl_6, $Zn(NO_3)_2 \cdot 6H_2O$, $HAuCl_4 \cdot 3H_2O$, and 5-bromosalicylic acid were purchased from Aladdin (Shanghai, China). Tripropylamine (TPA) was purchased from Maikelin (Beijing, China). Ethyl alcohol, polyvinylpyrrolidone (PVP), ascorbic acid (AA), and N,N-dimethylformamide (DMF) were purchased from Xilong Chemical Co., Ltd. (Guangdong, China). Bovine serum albumin (BSA) was purchased from Beijing Solarbio Science Technology Co., Ltd. (Beijing, China). Tris(2,2'-bipyridyl)ruthenium(II) chloride hexahydrate ($Ru(bpy)_3Cl_2 \cdot 6H_2O$) was purchased from Beijing InnoChem Science & Technology Co., Ltd. (Beijing, China). $NaBH_4$ was purchased from Shanghai Tianlian Fine Chemical Engineering Co., Ltd. (Shanghai, China). Hydrochloric acid was obtained from Guangdong Fine Chemical Engineering Technology Research and Development Center (Guangzhou, China). Alpha-fetoprotein (AFP), carcinoembryonic antigen (CEA), squamous cell carcinoma antigen (SCCA), NSE, and NSE antibodies were purchased from Beijing Boaosen Biotechnology Co., Ltd. (Beijing, China). CYFRA21-1 and CYFRA21-1 antibodies were purchased from Guangxi Jiaye Technology Co., Ltd. (Nanning, China). The human serum samples were supplied by the Guilin Fifth People's hospital. Phosphate buffer solutions (PBS, pH 7.4) were prepared by mixing solutions of 0.1 mol/L Na_2HPO_4 and 0.1 mol/L NaH_2PO_4. All other chemicals in the experiments were analytical grade. Double-distilled water (DDW) was used throughout the experiments.

Apparatus. The ECL experiments were performed using an MPI-B electrochemiluminescence detector at room temperature (Remex, China). A dual-disk glassy carbon electrode (DDGCE) was utilized as the working electrode. An Ag/AgCl electrode and a platinum wire served as the reference and counter electrodes,

respectively. Surface morphological images were gained by a model Vario Micro Cube scanning electron microscopy (SEM) (Elementar Company, Germany). Electrochemical experiments were recorded on a CHI 660 electrochemical workstation (Chenhua Instrument Co. Ltd., Shanghai, China). Transmission electron microscopy (TEM) images were obtained with a Tecnai G2 F20 S-TWIN transmission electron microscope (FEI Co., Hillsboro, OR, USA). X-ray powder diffraction patterns were obtained using a D/max-2500V/PC power X-ray diffractometer (Rigaku Corp., Tokyo, Japan) with Cu Kα radiation. Fluorescence spectra were obtained on a RF-5301 fluorescence spectrometer (Shimadzu, Japan).

Synthesis of SnS_2@Pt. First, 3D SnS_2NFs were synthesized by a previously reported hydrothermal method with some modification.[1] In brief, 40 mg $SnCl_4 \cdot 5H_2O$ and 40 mg TAA were dissolved into a beaker containing 25 mL PEG through ultrasonication. Then the mixture solution was transferred to a 50 mL Teflon-lined stainless-steel autoclave. The autoclave was heated at 180 ℃ for 12 h. After natural cooling, the precipitate was collected by centrifugation and washed with DDW and ethanol three times. The final product was dried at 70 ℃ for 12 h, and SnS_2NFs of dark brown power was obtained. 2 mg of SnS_2NFs were dissolved in 1 mL DDW, then 10 mg PVP and 2 mL 2% H_2PtCl_6 were added into the above solution. The mixture was maintained by moderately stirring for 12 h. After that, 14 mL of sodium citrate and 10 mg of $NaBH_4$ were added into the mixture and remained stirring for 12 h. The SnS_2@Pt composites were separated via centrifugation and further purified by washing with DDW.

Preparation of SnS_2@Pt/Ab_1. 1 mg SnS_2@Pt was dispersed into 1 mL of PSB (pH 7.4). A 500 μL, 1 μg/mL Ab_1 of NSE was added to the above solution under continuous stirring, and the mixture was allowed to react overnight. Then centrifugation was used to remove excess Ab_1 and the precipitate was re-dispersed into 1 mL of PBS (pH 7.4). A 150 μL 1% BSA was added to the mixture and reacted

for 6 h to closed non-specific binding sites. Then centrifugation removed unreacted BSA and the final precipitate was re-dispersed into PBS (pH7.4) and stored at 4 ℃ for the next stage of experiments.

Synthesis of $Ru(bpy)_3^{2+}$/Zn-MOF. Zinc oxalate MOFs were prepared according to literature reported previously[2] with a minor modification. In brief, 15 mg $Ru(bpy)_3Cl_2 \cdot 6H_2O$ and 100 mg $Zn(NO_3)_2 \cdot 6H_2O$ were added into a beaker. Subsequently, the mixture containing 30 mL DMF and 15 mL DDW were added into the beaker. Then 3 mL of HCl (3 mol/L) and 300 μL of oxalic acid (0.75 mol/L in DMF) were added into the above mixture. After ultrasonication for 10 min, the mixture was transferred to a round-bottom flask and reacted for 24 h at 60 ℃. The product was centrifuged and washed with DMF, ethanol, and DDW three times, respectively. Finally, the orange-colored $Ru(bpy)_3^{2+}$/Zn-MOF was obtained.

Synthesis of $Ru(bpy)_3^{2+}$/Zn-MOF/Ab_1. 1 mg $Ru(bpy)_3^{2+}$/Zn-MOF was suspended in 1 mL PBS by ultrasonication to obtain a homogeneous suspension. The 500 μL EDC (20 mmol/L) and NHS (10 mmol/L) were injected into the above mixture and reacted at 4 ℃ for 2 h. After that, 500 μL of 1 μg/mL Ab_1 of CYFRA21-1 was added into the above mixture and stirring continued for 12 h to allow binding on the surface of Zn-MOF via the amide reaction. Then 150 μL of 1% BSA were added to the mixture and reacted for 6 h to closed non-specific binding sites. The obtained $Ru(bpy)_3^{2+}$/Zn-MOF/Ab_1 hybrid was collected by centrifugation and further purified by washing with PBS solution and stored at 4 ℃ when not in use.

Syntheses of AuNRs. The preparation of AuNRs was according to literature via the seed-mediated surfactant-directed method with a slight improvement.[3] First, Au seeds were prepared. $HAuCl_4 \cdot 3H_2O$ (2 mL, 0.5 mmol/L) was added into a CTAB (5 mL, 0.2 mol/L) solution with sufficient mixing. Then, the ice-cold, freshly prepared $NaBH_4$ (0.6 mL, 0.01 mol/L) was quickly added with magnetic stirring for 2 min. Subsequently, the solution (Au seeds) was aged at ambient temperature for 2 h for later use.

The growth solution was prepared as follows. First, 0.8747 g CTAB and 0.1052 g 5-bromosalicylic acid were dissolved in 40 mL of DDW. Subsequently, the freshly

prepared $AgNO_3$ (1.5 mL, 4 mmol/L) was added into the solution and maintained undisturbed for 15 min at room temperature. Then 30 mL of 1 mmol/L $HAuCl_4 \cdot 3H_2O$ was added into the solution. The solution was adjusted to a pH of 1.3 by adding 2 mol/L HCl solution, dropwise, and stirred for 15 min. Next, 2 mL of 0.064 mol/L AA was injected into the above solution and stirred until it became colorless. Finally, 0.07 mL of the Au seeds solution was added into the growth solution with stirring for 30 s. The final solution was kept undisturbed for 4 h at room temperature. The solution gradually changed from colorless to a purple/red, which indicated that AuNRs were successfully prepared. The obtained product was centrifuged and washed with DDW.

Preparation of AuNRs/Ab_2. 1 mL of the AuNRs (1.5 mg/mL) was mixed with 5 μL of 10% Tween 20 and kept stirring for 30 min. After centrifugation, the product was dispersed in 1 mL of PBS (pH7.4). Subsequently, 450 μL Ab_2 of NSE was added into the above solution and incubated at 37 ℃ for 2 h. After centrifugation and washing with 0.1 mol/L PBS, the resulting product was dissolved in 1 mL of PBS containing 0.1% BSA and incubated at 37 ℃ for 1 h. The anti-NSE-AuNRs were eventually obtained by re-dispersing the conjugate in 1 mL of PBS after centrifugation. The anti-CYFRA21-1-AuNRs were prepared according to the same procedure.

Preparation of the ECL immunosensor. According to previous literature, the DDCE was separated into two spatial-resolved areas spaced 2 mm apart to avoid the cross-talk of the two areas.[4] Then, the DDGCE was polished with 0.3 and 0.05 μm alumina powder in sequence and washed with ethyl alcohol and DDW to make the surface of the electrode mirror-like. Then 3 μL SnS_2@Pt/Ab_1 and 3 μL $Ru(bpy)_3^{2+}$/Zn-MOF/Ab_1 were dropped onto the cleaned disks I and II of the DDGCE, respectively. The decorated DDGCE was dried in air. For NSE and CYFRA21-1 detection, 4 μL of NSE and CYFRA21-1 were dropped onto disks I and II of the decorated DDGCE for reacting for 1 h, respectively. Then the modified disks I and II were, respectively, incubated with 3 μL of anti-NSE-AuNRs and anti-CYFRA21-1-AuNRs for 1 h. The ECL measurement of the immunosensor was performed in 0.1 mol/L PBS (pH 7.4) containing 60 mmol/L $K_2S_2O_8$ and 1 mmol/L TPA. The

photomultiplier tuber (PMT) voltage was set at 800 V. The sweeping potential was set between -2.0 and 1.25 V with a scan rate of 0.1 V/s.

Optimization of experimental conditions.

Experimental conditions can affect the ECL performance for immunosensors, the pH of PBS, the luminophores concentrations of SnS_2@Pt and $Ru(bpy)_3^{2+}$/Zn-MOF, the concentration of $K_2S_2O_8$ and TPA, the concentration of AuNRs and the potential of ECL were optimized. As shown in Fig. S3A, pH influence was investigated, and the maximum ECL responses were obtained at pH 7.4. Therefore, pH 7.4 was selected as the optimum pH in the detection cell. The effect of the concentrations of SnS_2@Pt and $Ru(bpy)_3^{2+}$/Zn-MOF on the ECL responses were investigated. As shown in Fig. S3B, with increasing the concentration of SnS_2@Pt from 0.6 to 1.0 mg/mL, the ECL signal of SnS_2@Pt reached the maximum value. However, the ECL signal decreased with the concentration of SnS_2@Pt over 1.0 mg/mL. This is due to excess negatively charged radical deposited on the electrode surface. As displayed in Fig. S3B, the ECL response of $Ru(bpy)_3^{2+}$/Zn-MOF increased with the concentration of $Ru(bpy)_3^{2+}$/Zn-MOF increase. However, when the $Ru(bpy)_3^{2+}$/Zn-MOF concentration was larger than 1.0 mg/mL, no obvious response enhancement was produced. Hence, 1.0 mg/mL was selected as the optimum concentration of $Ru(bpy)_3^{2+}$/Zn-MOF. Fig. S3C displays the effect of the concentration of $K_2S_2O_8$ and TPA on the ECL signals of SnS_2NFs and $Ru(bpy)_3^{2+}$, respectively. As seen, the ECL response of SnS_2NFs showed a growing trend with the increase of the concentration of $K_2S_2O_8$ from 30 to 60 mmol/L. Afterwards, the ECL response of SnS_2NFs decreased as the $K_2S_2O_8$ concentration increased. Therefore, 60 mmol/L was selected as the optimum concentration of $K_2S_2O_8$. Fig. S3C displays the effects of TPA concentration on ECL of $Ru(bpy)_3^{2+}$ encapsulated in the Zn-MOF. The ECL intensity of $Ru(bpy)_3^{2+}$ reached a maximum value when the concentration of TPA was 1 mmol/L. The quantity of AuNRs was also optimized as displayed in Fig. S3D. The ECL responses reached a plateau when the concentration of AuNRs was 1.5 mg/mL, suggesting that the ECL-RET reached its highest efficiency. Therefore, 1.5 mg/mL of AuNRs was employed for further study.

The effect of potential on the ECL signal of $Ru(bpy_{)3}^{2+}$ was investigated by varying from 1.05 to 1.45 V. As presented in Fig. S3E, the ECL signal of $Ru(bpy)_3^{2+}$ reached its strongest value when the potential was 1.25 V. Therefore, 1.25 V was chosen as the optimal potential of modified disks II of the DDGCE. Similarly, the effect of potential on the ECL response of SnS_2NFs was investigated between -1.2 to -2.0 V. Simultaneously, the ECL response of SnS_2NFs reached its maximum value when the potential was -1.6 V. Therefore, -1.6 V was employed as the optimum potential of modified disks I of the DDGCE.

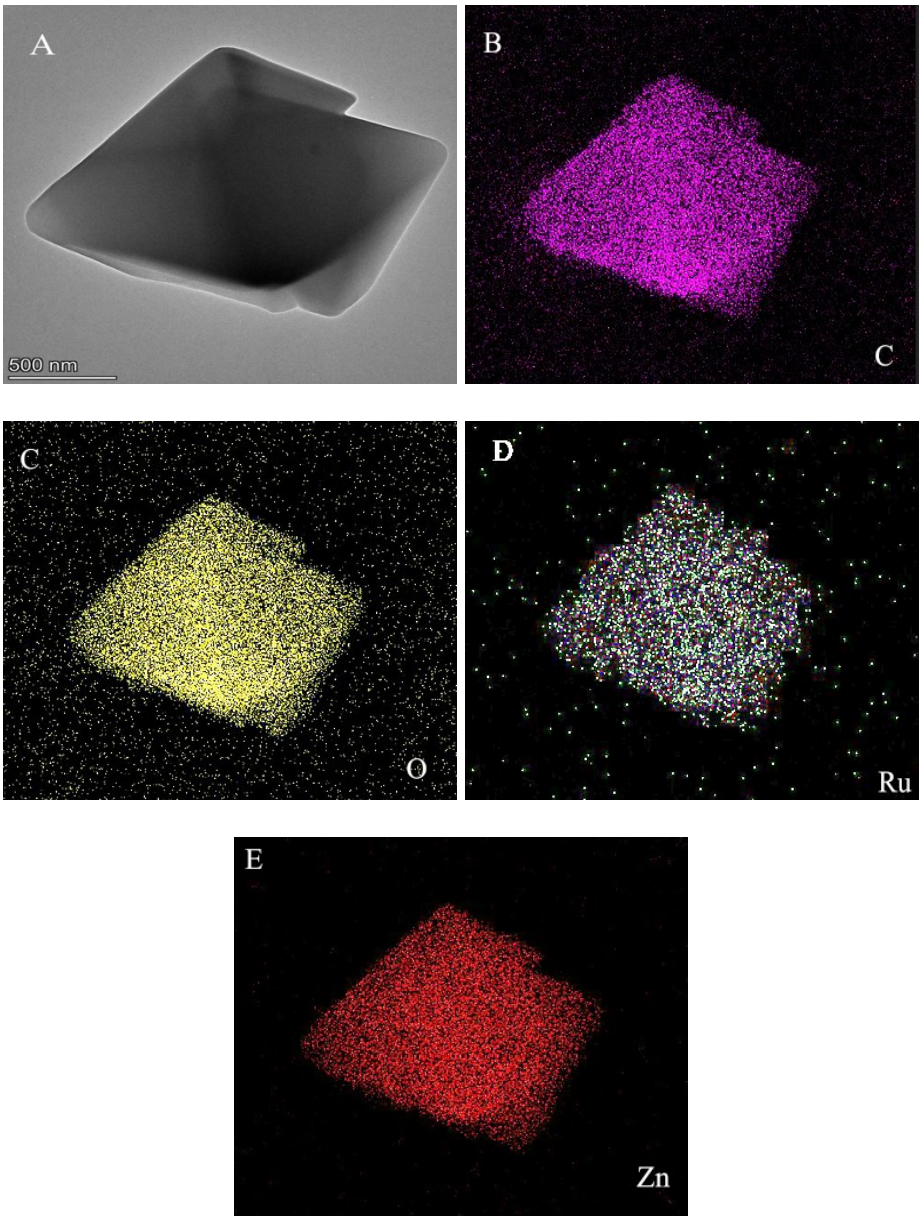

Fig. S1 (A) TEM image of $Ru(bpy)_3^{2+}$/Zn-MOF. (B-E) TEM-EDS mapping of (B) C, (C) O, (D) Ru and (E) Zn of the single $Ru(bpy)_3^{2+}$/Zn-MOF shown in (A).

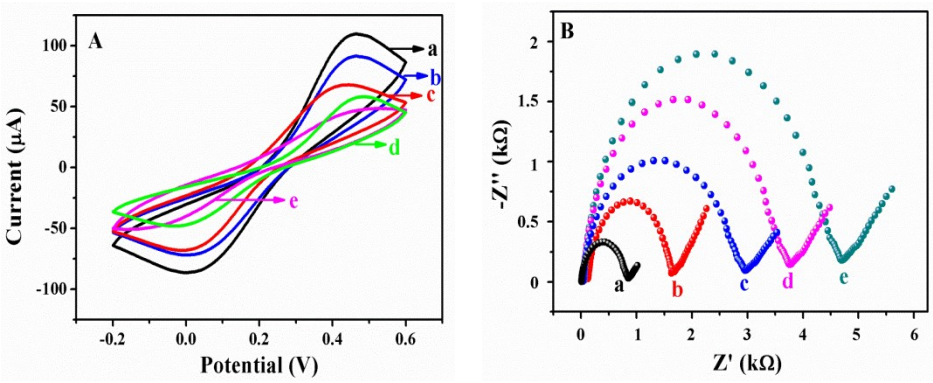

Fig. S2 (A) CV and (B) EIS of the stepwise fabrication process of the immunosensor (a) bare DDGCE, (b) SnS_2@Pt/Ab_1/GCE (disk I) and Ru(bpy)$_3^{2+}$/Zn-MOF/Ab_1/GCE (disk II), (c) SnS_2@Pt/Ab_1/BAS/GCE (disk I) and Ru(bpy)$_3^{2+}$/Zn-MOF/Ab_1/BSA/GCE (disk II), (d) SnS_2@Pt/Ab_1/BSA/NSE/GCE (disk I) and Ru(bpy)$_3^{2+}$/Zn-MOF/Ab_1/BSA/CYFRA21-1/GCE (disk II), (e) SnS_2@Pt/Ab_1/BSA/NSE/AuNRs/Ab_2/GCE (disk I) and Ru(bpy)$_3^{2+}$/Zn-MOF/Ab_1/BSA/CYFRA21-1/AuNRs/Ab_2/GCE (disk II).

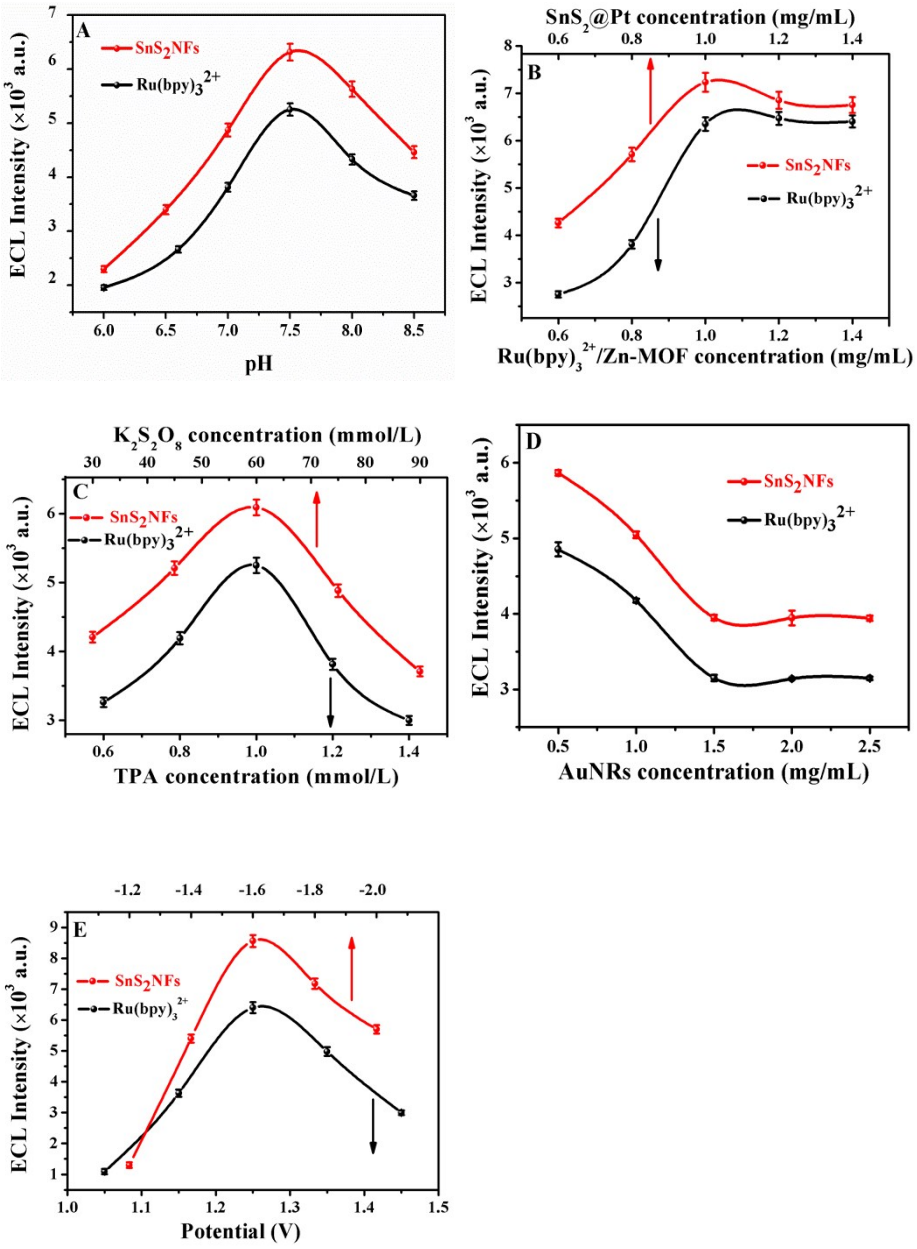

Fig. S3 Effects of (A) the pH of PBS, (B) the concentrations of SnS_2@Pt and $Ru(bpy)_3^{2+}$/Zn-MOF, (C) the concentrations of $K_2S_2O_8$ and TPA, (D) the concentration of AuNRs and (E) the potential on the ECL intensity.

Table S1 Comparison of Different Methods for NSE and CYFRA21-1 Detection

Method	CYFRA21-1			NSE		
	Linear range (ng/mL)	Detection limit (pg/mL)	Reference	Linear range (ng/mL)	Detection limit (pg/mL)	Reference
FL	1.3-480	160	5	1.25-80	625	9
EC	0.25-800	100	6	1-500	10	10
SERS	0.05-80	40	7	1-50000	860	11
MAIA	1.03-111	970	8	9.26-1000	37	8
ECL	0.00125-12.5	0.43	This work	0.0002-20	0.079	This work

Table S2 Analytical Results for NSE and CYFRA21-1 in Human Serum

NSE					CYFRA21-1				
Found (ng/mL)	Added (ng/mL)	Total found (ng/mL)	Recovery (%)	RSD (%)	Found (ng/mL)	Added (ng/mL)	Total found (ng/mL)	Recovery (%)	RSD (%)
1.482	1.000	2.474	99.20	3.5	0.4775	0.1250	0.5975	96.00	2.6
	2.000	3.504	101.1	1.7		0.2500	0.7332	102.3	3.9
	4.000	5.592	102.8	1.4		1.250	1.755	102.2	3.6
2.272	1.000	3.315	104.3	1.5	0.6201	0.1250	0.7425	97.92	2.8
	2.000	4.246	98.70	3.7		0.2500	0.8826	105.0	1.3
	4.000	6.430	103.9	1.8		1.250	1.911	103.3	2.1
2.516	1.000	3.492	97.60	1.6	0.9225	0.1250	1.052	103.6	4.1
	2.000	4.566	102.5	2.2		0.2500	1.165	97.00	3.4
	4.000	6.608	102.3	1.9		1.250	2.237	105.2	2.8

References

1 J. Xue, L. Yang, H. Wang, T. Yan, D. Fan, R. Feng, B. Du, Q. Wei and H. Ju, Biosens. Bioelectron. 2019, **133**, 192-198.

2 G. Zhao, Y. Wang, X. Li, Q. Yue, X. Dong, B. Du, W. Cao and Q. Wei, Anal. Chem. 2019, 91, 1989-1996.

3 J. Cao, F. Liu, X. Fu, J. Ma, S. Ren and Y. Liu, Chem. Commun. 2019, **55**, 2829-2832.

4 Y. Wang, F. Liu, J. Cao, S. Ren and Y. Liu, Biosens. Bioelectron. 2018, **102**, 525-530.

5 Z. Chen, R. Liang, X. Guo, J. Liang, Q. Deng, M. Li, T. An, T. Liu and Y. Wu, Biosens. Bioelectron. 2017, **91**, 60-65.

6 Y. Zeng, J. Bao, Y. Zhao, D. Huo, M. Chen, M. Yang, H. Fa and C. Hou, Talanta 2018, **178**, 122-128.

7 W. Lu, Y. Wang, X. Cao, L. Li, J. Dong and W. Qian, New J. Chem. 2015, **39**, 5420-5430.

8 L. Liu, S. Wu, F. Jing, H. Zhou, C. Jia, G. Li, H. Cong, Q. Jin and J. Zhao, Biosens. Bioelectron. 2016, **80**, 300-306.

9 Z. Cao, H. Li, C. Lau and Y. Zhang, Anal. Chim. Acta 2011, **698**, 44-50.

10 F. Yan, J. Liu, Y. Wang, J. Luo, H. Xu, S. Xu and X. Cai, Biosens. Bioelectron. 2017, **95**, 60-66.

11 X. Gao, P. Zheng, S. J. Kasani, S. Wu, F. Yang, S. Lewis, S. Nayeem, E. B. Engler-Chiurazzi, J. G. Wigginton, J. W. Simpkins and N. Q. Wu, Anal. Chem. 2017, **89**, 10104-10110.